An Effective Two-Component Description of Colloid−Polymer Phase Separation

Andrea Pelissetto*

Dipartimento di Fisica and INFN - Sezione di Roma I, Università degli Studi di Roma "La Sapienza", P. le A. Moro 2, I-00185 Roma, Italy

Jean-Pierre Hansen†

Department of Chemistry, Lensfield Road, Cambridge CB21EW, U.K.

Received July 26, 2006; Revised Manuscript Received October 9, 2006

ABSTRACT: Effective pair potentials $v(r)$ between hard-sphere colloids and the centers of mass of self-avoiding polymer coils are determined in the low-density limit by Monte Carlo sampling of polymer conformations, over a wide range of size ratios $\lambda = R_c/R_g$, where R_c and R_g are the colloid and polymer radii. In the protein limit $\lambda \ll 1$, $v(r)$ is small compared to the thermal energy k_BT, allowing the use of thermodynamic perturbation theory within the effective two-component representation to determine the free energy of colloid−polymer mixtures and the resulting segregation line. In the opposite limit ($\lambda > 1$), the effective interaction $v(r)$ develops a hard core, preventing the application of standard thermodynamic perturbation theory. A variant on the latter, focusing on the Mayer *f*-function, rather than on the effective colloid−polymer potential, allows the extension of the perturbative calculations to all size ratios λ. The predicted phase diagrams are in semiquantitative agreement with available simulation data, both in the protein ($\lambda < 1$) and in the colloid ($\lambda > 1$) regimes.

I. Introduction

The mesoscopic structure, phase behavior, and rheology of colloidal suspensions are strongly altered by the addition of nonadsorbing polymers. The key mechanism underlying these changes in static and dynamic properties is polymer depletion linked to the observation that individual polymer segments cannot penetrate the compact colloidal particles. This leads to a reduction of the allowable polymer conformations in the vicinity of the colloid; the concomitant loss in entropy can trigger segregation into colloid-rich (or *colloid liquid*) and colloid-poor (or *colloid gas*) phases.

In the following, as in much of the existing literature, restriction will be made to hard spherical colloidal particles of radius R_c. The mean polymer size is best characterized by the radius of gyration R_g of the individual polymer coils. Apart from the practical aspects of the material properties of colloid−polymer mixtures, the statistical mechanics of binary systems involving both rigid and deformable particles constitutes an interesting and challenging problem.

A crucial parameter characterizing such mixtures is the size ratio $\lambda \equiv R_c/R_g$. In many practical situations the colloidal particles are substantially larger than polymer coils so that $\lambda > 1$. In fact, the case $\lambda \gg 1$ is frequently referred to as *colloid limit*. It has been thoroughly investigated following the pioneering work of Asakura and Oosawa[1] and Vrij[2] and is well understood.[3] Polymer conformation fluctuations play a relatively minor role and the smaller polymer coils induce depletion-driven, mostly pairwise-additive attractive interactions between the larger colloids. This attraction induces a colloid *liquid*−*gas* transition for sufficiently high polymer concentration. There are quantitative and even qualitative differences between the phase diagrams resulting from ideal or interacting polymer chains,[4] but the basic depletion picture remains the same.

* Corresponding author. E-mail: Andrea.Pelissetto@roma1.infn.it.
† E-mail: jph32@cam.ac.uk.

The case $\lambda < 1$ is less well understood. Conformational changes now play an important role since the larger polymer can wrap around the smaller colloids. Experimental data for mixtures of polymers and proteins,[4,5] micelles,[6] and silica nanoparticles[7] all give clear evidence of phase separation over a system-dependent range of polymer and colloid concentrations. The term *protein limit* has been coined for the regime $\lambda \ll 1$, since it can be achieved by mixtures of small globular proteins and high molecular-weight polymers. The biological interest in such mixtures arises from the observation that the addition of water-soluble polymers to protein solutions favors protein crystallization, a notoriously difficult but crucial step toward the X-ray determination of their structure.

A number of theoretical investigations of the structure, thermodynamics, and phase behavior of colloid−polymer systems with $\lambda < 1$ have been reported, leading to sometimes conflicting predictions. They may be broadly classified as belonging to one of three levels of description:

(a) Full, monomer-level approaches allow for a detailed description of polymer conformations in the presence of one or several hard-sphere colloidal particles. These include, among others, the field-theoretic investigations of Eisenriegler and collaborators,[8] the fluid integral-equation calculations of Schweizer and co-workers[9] based on the polymer reference interaction-site model (PRISM), as well as Monte Carlo (MC) simulations involving lattice models of ideal[10] and interacting[11] polymers. Provided the intrinsic limitations of such simulations (e.g., the limited range of polymer lengths) are kept in mind, they provide stringent benchmarks against which approximate theories for equivalent models must be gauged.

(b) Within a reductionist strategy, whereby individual monomer degrees of freedom are averaged out, the initial colloid−polymer mixture may be mapped onto a much simpler effective two-component system involving only effective interactions between the centers of mass (CMs) of the colloidal hard spheres and of the polymer coils regarded as *soft colloids*[12] in the spirit

10.1021/ma061690f CCC: $33.50
Published on Web 11/30/2006

of the Asakura−Oosawa model.[13] This approach has proved to be very successful for pure solutions of interacting polymers[12,14] and for colloid−polymer mixtures in the large-colloid regime ($\lambda > 1$),[15] but has so far been less exploited in the small-colloid regime ($\lambda < 1$). The Asakura−Oosawa model has been extended to the latter regime[16] and so has the successful free-volume theory of Lekkerkerker et al.,[16,17] while Sear has proposed an interesting generalization of the Asakura−Oosawa model to the protein limit, where the depletant is identified with polymer *blobs*[18] of a size similar to that of the colloids, rather than the larger full polymer coil.[19]

(c) One may attempt one further step in the coarse-graining strategy by reducing the initial two-component problem to an effective one-component system of colloidal particles interacting via polymer depletion-induced effective interactions. This approach has proved rather fruitful in the large-colloid regime ($\lambda > 1$)[20,21] but has been shown to be useless in the protein limit ($\lambda < 1$) due to the growing importance of many-body interactions compared to the effective pair interactions.[10,11,16,22] As anticipated by de Gennes,[23] the effective pair interactions are too weak to induce the observed partitioning of small colloids in the presence of large polymers and cumbersome many-body interactions would have to be included to lead to phase separation, thus rendering the effective one-component representation untractable.

In the present paper, we return to the effective two-component representation, in an attempt to extend it to arbitrary values of the size ratio λ, including the less-studied protein limit. To that purpose we first compute the effective pair potential between a hard-sphere colloid and the CM of a single interacting polymer over a wide range of size ratios ($0.02 \le \lambda \le 10$) and of polymer lengths L (section 2). Following our earlier work on effective polymer−polymer pair potentials[24] we investigate the scaling limit ($L \to \infty$) and finite-length corrections to the colloid−polymer potentials. For $\lambda \ll 1$, the effective polymer−colloid coupling is sufficiently weak to justify the use of standard thermodynamic perturbation theory for the calculation of the free energy of colloid−polymer mixtures, as well as the resulting phase diagram. This perturbation theory is no longer applicable when $\lambda \gtrsim 0.5$, because the effective colloid−polymer pair potential becomes much larger than the thermal energy k_BT at short center-to-center distances. A variant of thermodynamic perturbation theory is formulated to handle strongly repulsive pair potentials, and is applied to the calculation of colloid−polymer phase diagrams over the whole range of size ratios λ (section 3). A discussion of possible extensions of the present approach and concluding remarks are given in section 4.

II. Effective Colloid−Polymer Potentials

The basic model considered throughout this paper is a mixture of hard spheres of radius R_c and polymers of length L *living* on a cubic lattice. The segment length b coincides with the lattice spacing and will serve as unit of length. The centers of the N_c spheres occupy one of the Ω lattice sites. The colloid number density is $\rho_c = N_c/\Omega$ and the corresponding volume fraction is $\varphi_c \equiv 4\pi\rho_c R_c^3/3$. The polymers are self- and mutually avoiding walks (SAWs), i.e., any lattice site can be occupied by at most one monomer; there is an attractive energy, $-\epsilon$ ($\epsilon > 0$) between nonbonded, adjacent monomers. The monomers are excluded from the nonoverlapping hard-sphere volumes. With N_p polymers on the lattice, their number density is $\rho_p = N_p/\Omega$, while the segment concentration is $c = L\rho_p$. The polymer volume fraction is conveniently defined in terms of the polymer radius of gyration R_g, $\varphi_p \equiv 4\pi\rho_p R_g^3/3$. The overlap density ($\rho_p^*$) is defined as the polymer density at which the volume per polymer $1/\rho_p$ equals the volume of one coil, i.e., $\varphi_p = \varphi_p^* = 1$. The corresponding monomer concentration $c^* = 3L/(4\pi R_g^3)$ scales like $L^{1-3\nu}$, where ν is the radius-of-gyration exponent ($R_g \sim L^\nu$); $\nu \approx 0.588$ in the good-solvent regime,[25] while $\nu = 1/2$ for ideal chains. Note that, at fixed φ_p, the monomer concentration vanishes in the scaling ($L \to \infty$) limit so that polymer coils in solution can easily interpenetrate.

It is customary to distinguish the dilute regime ($\rho_p < \rho_p^*$) from the semidilute regime ($\rho_p > \rho_p^*$). In the former the only relevant polymer length scale (for a given segment length b) is the radius of gyration R_g, whereas in the latter regime a second length scale, characterizing the network of interpenetrating polymers, comes into play, namely the correlation length:[18]

$$\xi \sim R_g \varphi_p^{-\nu/(3\nu-1)} \tag{2.1}$$

In an athermal ($\epsilon = 0$) colloid−polymer mixture the key physical parameters are the ratio $\lambda \equiv R_c/R_g$, the volume fractions φ_c and φ_p, and the polymer length L (note that the ratio $\lambda_\xi = R_c/\xi$ is determined by λ and eq 2.1). If monomer−monomer attractions are present ($\epsilon = 0$), there is an additional inverse temperature variable $\beta^* \equiv \beta\epsilon = \epsilon/k_BT$. In a θ solvent a single chain contracts to an ideal chain ($\nu = 1/2$); in the present model the inverse-temperature parameter β^* takes the value $\beta_\theta^* \simeq 0.2687$ in the scaling limit.[26]

In this section we consider the infinite-dilution limit (φ_c, $\varphi_p \to 0$); in the spirit of the effective two-component representation, we first determine the effective pair potential between the CMs of an isolated pair of one colloid and one polymer as a function of the distance r between their CMs. If $H(1, 2)$ is the total interaction energy between a colloid with CM at $\mathbf{r}_2$ and a polymer coil with CM at $\mathbf{r}_1$, then the effective pair potential is defined as

$$\beta v_2(r; L, R_c;\beta) \equiv -\ln\langle e^{-\beta H(1,2)}\rangle_r \tag{2.2}$$

where $r \equiv |\mathbf{r}_1 - \mathbf{r}_2|$ and the average is taken over all polymer conformations such that the distance between the colloid and the polymer CMs is r. In the lattice model, the sum over conformations reduces to a sum over all walks of length L. In the scaling limit ($L \to \infty$ at fixed λ), like any invariant universal ratio of statistical polymer properties, $\beta v_2(r;L, R_c;\beta)$ goes over to a universal function $v_\infty(x;\lambda)$ of λ and of a reduced CM−CM distance $x \equiv r/R_s$. For R_s, we have chosen the length $R_s = \sqrt{(R_c^2 + R_g^2)}$. For large, but finite polymer length L, corrections to the scaling limit lead to the following expression:[24,27,28]

$$\beta v_2(r; L, R_c;\beta) = v_\infty(x;\lambda) + a_v(\beta) v_c(x;\lambda) L^{-\Delta} + b_v(x;\beta,\lambda) L^{-\Delta_{\rm eff}} + \cdots \tag{2.3}$$

with the normalization condition $v_c(0;1) = 1$; $a_v(\beta)$ is a nonuniversal temperature-dependent amplitude. The most accurate estimate of the exponent Δ so far yields[25] $\Delta = 0.515 \pm 0.017$. The last term with $\Delta_{\rm eff} \approx 1$ is an effective correction term that corresponds to the sum of three (or more) terms with exponent close to 1.[24]

The second virial coefficient for a colloid−polymer pair is defined as

$$B_2(L, R_c;\beta) = \frac{1}{2}\int d^3\mathbf{r}_1 \langle 1 - e^{-\beta H(1,2)}\rangle_{0,\mathbf{r}_1} \tag{2.4}$$

where the average is over all walks of length L starting at the

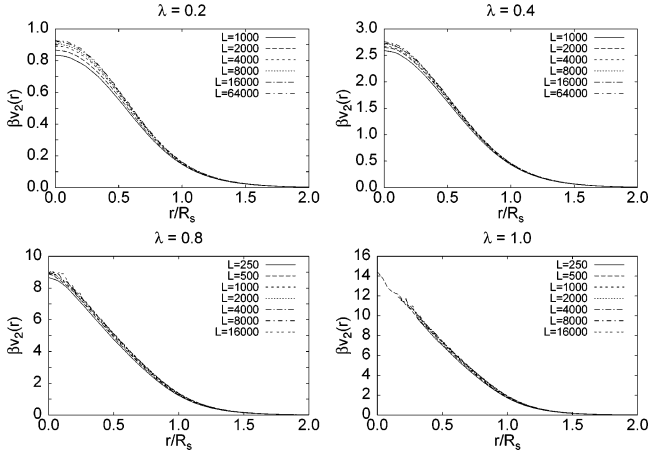

Figure 1. Effective pair potential $\beta v_2(r;L, R_c;\beta)$ vs $x = r/R_s$ for several values of λ and L. Here $\beta^* = 0$.

origin, while a colloid is placed at $\mathbf{r}_1$. The universal ratio

$$A_2(L, R_c;\beta) = \frac{B_2(L, R_c;\beta)}{[R_g(L,\beta)]^{3/2} R_c^{3/2}} \tag{2.5}$$

may be expressed in a form similar to eq 3 in the scaling limit:

$$A_2(L, R_c;\beta) = A_2^{\infty}(\lambda) + a_2(\beta) f_2(\lambda) L^{-\Delta} + b_2(\beta,\lambda) L^{-\Delta_{\text{eff}}} + \cdots \tag{2.6}$$

with the normalization $f_2(1) = 1$. A careful finite-size-scaling analysis, similar to that carried out in ref 24 for the case of two identical polymers, allows in principle $v_\infty(x;\lambda)$, $v_c(x;\lambda)$, $A_2^{\infty}(\lambda)$, $f_2(\lambda)$, as well as the universal amplitude ratio $a_i(\beta)/a_2(\beta)$ to be extracted from accurate MC simulations carried out for several lengths L.

We have carried out such simulations over a wide range of size ratios, $0.02 \le \lambda \le 10$, covering both the protein and the colloid regimes. We used the pivot algorithm[29−32] (together with bilocal moves[33] and the multiple Markov chain method[34,35] close to the Θ point) and simulated walks with L varying between 100 and 64000.

We have first considered the pair potential $\beta v_2(x;L, R_c;\beta)$ and determined the scaling functions $v_\infty(x;\lambda)$ and $v_c(x;\lambda)$. For this purpose the effective pair potential is required for several values of L at the *same* value of λ. This condition cannot be fulfilled directly: since R_c can only be an integer multiple of the lattice spacing b, only a discrete set of λ can be generated for any given L. To obtain results at a fixed value of λ, we have first determined the effective pair potential at two nearby values λ_1 and λ_2, and then we have performed a linear interpolation. This correction is quantitatively small when R_c/b is large, since in this case one can choose R_c in such a way to obtain a good approximation of the desired λ, but is crucial when R_c/b is small, e.g., 3−5. In Figure 1 we show the results for $\lambda = 0.2$, 0.4, 0.8, and 1, for different values of L and $\beta^* = 0$. The L dependence is significant for $\lambda \lesssim 0.5$, but the scaling limit is rapidly reached for $\lambda > 0.5$. This is partly a consequence of discretization: scaling corrections are small only if $R_c/b \gg 1$, i.e., for $L \gg \lambda^{-1/\nu}$. Therefore, very long polymer chains are required in the limit of small λ. In practice, discretization corrections appear to be small for $R_c/b \gtrsim 5$; this required us to simulate walks of length $L = 64\,000$ ($R_g/b \approx 300$) to obtain reliable results down to $\lambda \approx 0.02$. The sphere-to-segment ratio has a nonnegligible influence on the monomer depletion layer thickness around a sphere.[36] In Figure 2, we show the predicted universal function

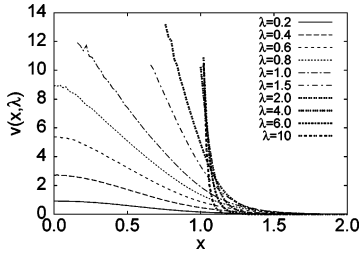

Figure 2. Effective pair potential in the scaling limit: universal function $v_\infty(x;\lambda)$ vs x for several values of λ.

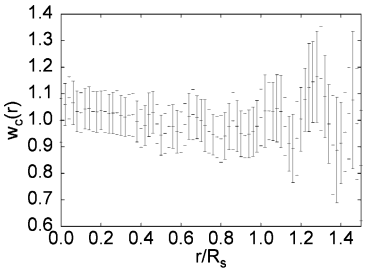

Figure 3. Scaling corrections to the effective pair potential: universal function $w_c(x;\lambda) = [v_c(x;\lambda)/v_c(0;\lambda)]/[v_\infty(x;\lambda)/v_\infty(0;\lambda)]$ vs x for $\lambda = 0.2$.

$v_\infty(x;\lambda)$. The main observations are that (i) the effective potentials are always repulsive, monotonically decreasing with x, and of short range; (ii) the maximum value $v_\infty(x = 0)$ is weak for the smallest values of λ, but increases rapidly with λ. Observation i is an immediate consequence of the fact that the scaling limit can be obtained by considering data with $\beta^* = 0$ and in this case the Boltzmann factor in eq 2.2 can only take the values 0 and 1. Observation ii reflects the fact that in the protein limit $\lambda \ll 1$ the polymer can wrap around the hard sphere, which becomes increasingly unlikely as the size ratio increases.

For $\lambda \lesssim 0.5$—the regime in which scaling corrections are sizable—we can determine the correction-to-scaling function $v_c(x,\lambda)$ using the method described in ref 24. There it was shown that the correction function $v_c(x)$ for the polymer−polymer effective pair potential was approximately proportional to $v_\infty(x)$, i.e., the ratio $v_c(x)/v_\infty(x)$ was independent of x within error bars. Within the precision of our MC data, the same constancy is roughly observed for $v_c(x)$ when $\lambda \lesssim 0.5$, as can be seen in Figure 3, where we report the ratio

$$w_c(x;\lambda) = \frac{v_c(x;\lambda)}{v_c(0;\lambda)} \times \frac{v_\infty(0;\lambda)}{v_\infty(x;\lambda)} \tag{2.7}$$

for $\lambda = 0.2$.

From the results reported in Figure 2 one can see that $v_\infty(x = 0;\lambda)$ increases rapidly as λ increases and no estimate is obtained for $\lambda > 1$, since in this case polymer conformations that wrap around the sphere become increasingly unlikely. The value $v_2(x = 0;L, R_c;\beta)$ is identical to the work required to insert a sphere into a single polymer coil. This was estimated by de Gennes[23] to scale like $\lambda^{3-1/\nu} \simeq \lambda^{1.30}$. To check this relation, we plot $f(\lambda, L) \equiv \beta v_2(0;L, R_c;\beta)/\lambda^{1.30}$ in Figure 4. If de Gennes' scaling is correct, $f(\lambda, L)$ should approach a finite constant as $L \to \infty$ followed by $\lambda \to 0$. The results support this conclusion and give $f(0;\infty) \approx 5.5$.

By using the blob picture one can relate $v_\infty(x;\lambda)$ for $\lambda \to 0$ with the scaling function associated with the monomer−CM distribution for a single polymer in the absence of the colloid. Indeed, if λ is small, the colloid interacts only with a polymer blob of length $L_1 \sim R_c^{1/\nu}$. Thus, we can write

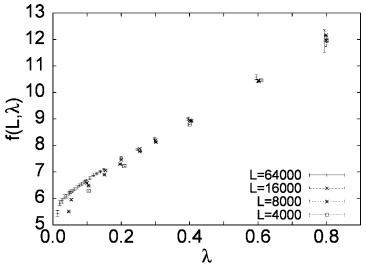

Figure 4. Function $f(\lambda, L;\beta)\equiv\beta v_2(0;L, R_c;\beta)/\lambda^{1.30}$ for $\beta^* = 0$ and several values of λ and L.

$$\beta v_2(r) \approx -\ln\{e^{-\beta V_{blob}} s^3 p_{bl}(r) + [1 - s^3 p_{bl}(r)]\} \quad (2.8)$$

where $p_{bl}(r)$ is the probability that there is a blob at a distance r from the CM, V_{blob} is the interaction energy between the blob and the colloid, and $s \sim R_c$ is the typical interaction distance between the polymer blob and the colloid. The probability $p_{bl}(r)$ satisfies the normalization condition

$$\int d^3\mathbf{r}\, p_{bl}(r) = N_{blobs} \quad (2.9)$$

where N_{blobs} is the number of blobs. For dimensional reasons we must have in the scaling limit

$$p_{bl}(r) = \frac{N_{blobs}}{R_g^3} p_{scal,bl}(r/R_g) \quad (2.10)$$

with

$$\int d^3\boldsymbol{x}\, p_{scal,bl}(x) = 1 \quad (2.11)$$

From eq 2.8 it follows that

$$\beta v_2(r) \approx -\ln\left[1 - (1 - e^{-\beta V_{blob}})\frac{s^3 N_{blobs}}{R_g^3} p_{scal,bl}(r/R_g)\right]$$

$$\sim \frac{s^3 N_{blobs}}{R_g^3} p_{scal,bl}(r/R_g) \quad (2.12)$$

where we used $s^3 N_{blobs}/R_g{}^3 \sim \lambda^{3-1/\nu} \to 0$ for $\lambda \to 0$. The prefactor follows from

$$B_2 = \frac{1}{2}\int d^3\boldsymbol{r}\, (1 - e^{-\beta v_2(r)}) \quad (2.13)$$

This gives the relation

$$\beta v_2(r) = \frac{2B_2}{R_g^3} p_{scal,bl}(r/R_g) \quad (2.14)$$

valid for $\lambda \to 0$ in the scaling limit. The function $p_{scal,bl}(x)$ can be related to the analogous universal function that characterizes the scaling behavior of the monomer-CM distribution function. Let $4\pi r^2 p_{CM}(r)\, dr$ be the number of monomers whose distance from the CM is between r and $r + dr$. In the scaling limit

$$p_{CM}(r) = \frac{L}{R_g^3} p_{scal,CM}(r/R_g) \quad (2.15)$$

We wish now to argue that $p_{scal,bl}(x) = p_{scal,CM}(x)$. Indeed, for $\lambda \to 0$ the blob size R_c is infinitely small compared to R_g, which is the relevant length scale in the scaling limit. Since $p_{scal,CM}(x)$ is universal, the same function characterizes the distribution of single monomers or of small blobs (in other words, $p_{scal,CM}(x)$ is invariant under a renormalization-group coarsening procedure in which "small" blobs are replaced by a single monomer). With this identification, since $R_g \approx R_s$ in the limit $\lambda \to 0$, we obtain

$$v_\infty(x;\lambda) = 2A_2^\infty(\lambda)\lambda^{3/2} p_{scal,CM}(x) \quad (2.16)$$

To verify this relation, we have computed numerically the function $p_{scal,CM}(x)$, and we have compared it with the ratio $\beta v_2(r)\lambda^{-3/2}/(2A_2)$; see Figure 5. The relation is verified quite accurately. Note that the derivation of relation 2.16 is quite general and relies only on the fractal nature of the polymer. Hence, it applies not only to SAWs, i.e., to polymers in the good-solvent regime, but also to ideal chains.

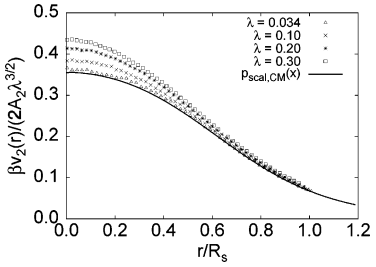

Figure 5. Plot of the ratio $\beta v_2(r;L, R_c;\beta)/[2A_2(L, R_c;\beta)\lambda^{3/2}]$ vs r/R_s for $L = 64\,000$, $\beta^* = 0$, and several values of λ. The continuous line corresponds to the function $p_{scal,CM}(x)$ defined in the text.

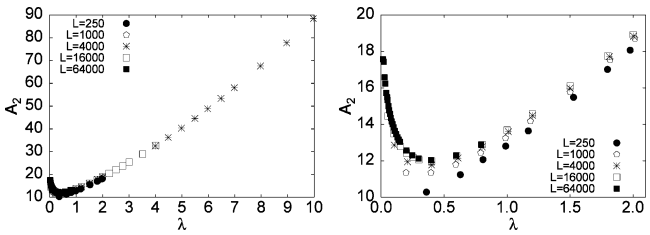

Figure 6. Second virial coefficient: plot of $A_2(L, R_c;\beta)$ vs λ for several values of L and $\beta^* = 0$. On the left we report all data for $\lambda \le 10$, on the right we only show the data for $\lambda \le 2$.

The second virial coefficient in the dimensionless form 2.5 is plotted in Figure 6 as a function of λ for several values of L. As in the case of βv_2, the L dependence of A_2 is seen to be substantial below $\lambda \le 1$, and to become much weaker for larger size ratios. A_2 goes through a minimum for $\lambda \simeq 0.4$ and rises steadily thereafter. The behavior for small and large values of λ can be understood by simple arguments. The behavior for small λ can be obtained by using once more the blob picture, in which the colloid interacts only with a polymer blob of length $L_1 \sim R_c{}^{1/\nu}$. Thus, $B_2 \approx (L/L_1)B_{2,blob} \sim \lambda^{-1/\nu} B_{2,blob}$. For dimensional reasons we expect $B_{2,blob} \sim R_c{}^3$, which implies $A_2^\infty \sim \lambda^{3/2-1/\nu} = \lambda^{-0.202}$. This result is consistent with the small-λ behavior of the pair potential, $v_\infty(x;\lambda) \sim \lambda^{3-1/\nu} v_{0,\infty}(x)$. The prefactor can be obtained from the results of ref 37 that give the free energy for the insertion of a single colloid: if A_g is the constant defined in ref 37 [see eq 1.4], $A_2^\infty = A_g \lambda^{3/2-1/\nu}/2$. Using the field-theoretical prediction $A_g \approx 18.4$, we thus expect $A_2^\infty \approx 9.2 \times \lambda^{3/2-1/\nu}$. To check this prediction, we plot $A_2\lambda^{0.202}$ in Figure 7. If we do not consider the data with $\lambda < 0.03$ which are probably affected by corrections to scaling, it is clear that $A_2\lambda^{0.202}$ converges to a constant as $\lambda \to 0$, confirming the predicted asymptotic behavior. As for the prefactor, our data indicate that $A_2\lambda^{0.202}$ converges to some number between 8 and 8.5 as $\lambda \to 0$, which is reasonably close to the field-theoretical prediction. For $\lambda \to \infty$, we expect B_2 to be proportional to $(R_c + R_g)^3$ and thus $A_2^\infty \sim \lambda^{-3/2}(1 + \lambda)^3$. The results shown in Figure 7

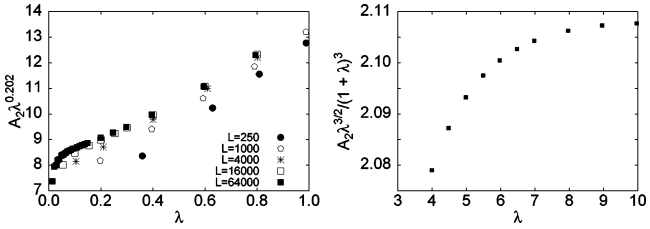

Figure 7. Second virial coefficient: on the left we show $A_2(L, R_c;\beta)\lambda^{0.202}$ vs λ for several values of L, on the right $A_2(L, R_c;\beta)\lambda^{3/2}/(1+\lambda)^3$ vs λ for $L = 4000$. In all cases $\beta^* = 0$.

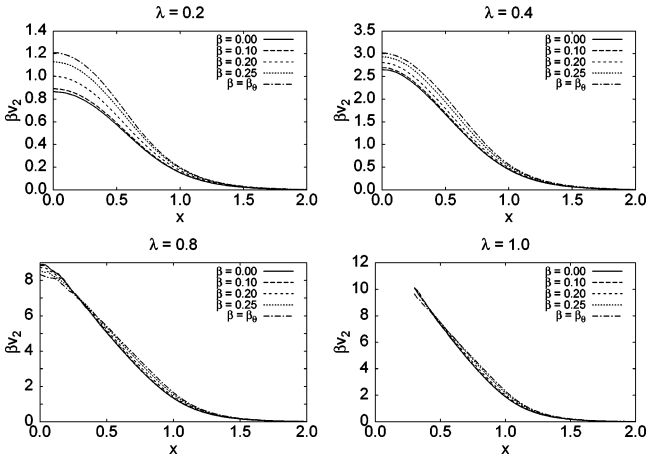

Figure 8. Effective pair potential vs $x = r/R_s$ for $L = 2000$ and several values of β^*, up to $\beta^*_\theta \approx 0.2687$.

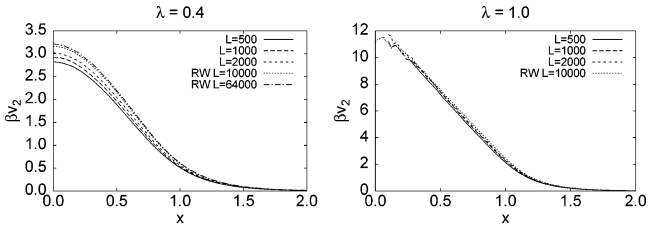

Figure 9. Effective pair potential for $\beta^* = 0.2687 \approx \beta^*_\theta$ and several values of L. For comparison we also report the effective pair potential for the ideal−polymer or random-walk (RW) case.

confirm this prediction and provide the prefactor. For $\lambda \to \infty$, we obtain $A_2^\infty \approx 2.11\lambda^{3/2}$.

We have also investigated the influence of monomer−monomer attraction ($\epsilon \neq 0$) on the effective pair potential $\beta v_2(x;L, R_c;\beta)$. Results for $0 \le \beta^* \le \beta^*_\theta$ are shown in Figure 8 for $L = 2000$. As might have been expected, the effective CM-CM interaction becomes more repulsive as β^* increases toward the θ regime. The observed increase of $\beta v_2(x = 0)$ is particularly strong for the smallest size ratios. It is due to the contraction of the polymer coil as β progressively increases which prevents the polymer to wrap around the sphere. The effect is less pronounced for larger size ratios and, for $\lambda \ge 1$, the effective potential is nearly independent of β. For $\beta \approx \beta_\theta$ and any fixed λ, βv_2 should converge to the effective pair potential between an ideal chain (random walk) and a colloid. The results reported in Figure 9 show that this indeed happens.

The temperature-dependent second virial coefficient in its reduced form 2.5 is illustrated in Figure 10 as a function of β^* for $L = 2000$ and several values of λ. As expected from the results for βv_2, A_2 increases with β^* for any given λ. We also show data at $\beta = \beta_\theta$ together with results for an ideal polymer chain: they are seen to lie slightly above the SAW

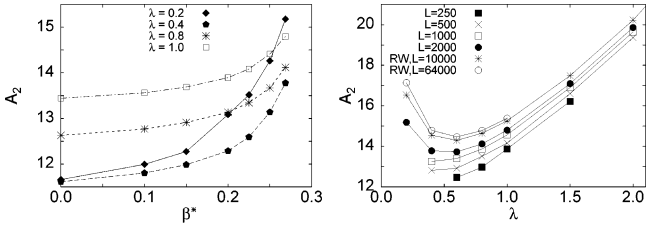

Figure 10. Second virial coefficient: on the left we report A_2 vs β^* for several values of λ; on the right A_2 vs λ for $\beta^* = 0.2687 \approx \beta^*_\theta$ for several values of L. For comparison we also report A_2 for the random-walk (RW) case.

Θ-temperature results. As expected the difference decreases as L increases.

In the following section, we are going to exploit the results obtained for βv_2 and A_2 to investigate possible colloid−polymer phase separation.

III. Colloid−Polymer Segregation

The results of the previous section show that the effective polymer−colloid pair potential $v_2(r)$ goes to zero as $\lambda \to 0$ and its maximum value $v_2(r = 0)$ does not exceed k_BT for $\lambda \lesssim 0.2$. It appears hence natural to apply theormodynamic perturbation theory[38] to compute the free energy of colloid−polymer mixtures in the protein limit, taking the two-fluid system of independent (decoupled) colloid and polymer components as a reference system. Such a perturbation theory is somewhat unusual, since, while polymers interact with polymers and colloids with colloids, particles of different species do not interact in the reference system. For $\lambda > 0.2$, on the other hand, $\beta v_2(r)$ increases rapidly beyond 1, and standard thermodynamic perturbation theory, which is essentially a cumulant expansion in powers of $\beta v_2(r)$, is no longer expected to converge. Moreover, for $\lambda \gtrsim 1$, $\beta v_2(r)$ develops a hard core, due to the fact that polymers are no longer able to wrap around the large hard-sphere colloids. We present here and in the Appendix a variant of thermodynamic perturbation theory, which amounts to an expansion in powers of the Mayer f function for a colloid−polymer pair. It allows one to circumvent the breakdown of traditional perturbation theory and to calculate free energies and the resulting phase diagram for any value of λ.

Let $f \equiv \beta F/N$ be the reduced free energy per particle of the mixture, where $N = N_1 + N_2$, N_1 and N_2 are the total numbers of polymers and colloids, and $x_1 = N_1/N$, $x_2 = N_2/N = 1 - x_1$ the corresponding number fractions. Then f may be expanded as

$$f = f^{(0)} + f^{(1)} + f^{(2)} + \cdots \tag{3.1}$$

where $f^{(0)} = f^{(0)}_{\text{pol}} + f^{(0)}_{\text{coll}}$ is the free energy of the reference system, i.e., the sum of the free energies of the polymer fluid and of the hard-sphere colloid fluid, while $f^{(1)}$ and $f^{(2)}$ are the first- and second-order corrections. Explicit expressions are given in the Appendix. The three terms on the rhs of eq 3.1 can be expressed in terms of the equations of state and of the pair correlation functions of the pure polymer and hard-sphere fluids. The colloid contribution to $f^{(0)}$ is taken from the accurate Carnahan−Starling equation of state of a hard sphere fluid[38]

$$f^{(0)}_{\text{coll}}(\rho_c) = x_2\left[\ln\rho_c + \frac{\varphi_c(4-3\varphi_c)}{(1-\varphi_c)^2}\right] \tag{3.2}$$

where the irrelevant de Broglie thermal wavelength was chosen equal to the unit of length.

The polymer contribution $f_{pol}^{(0)}$ to the reference free energy can be derived from the polymer equation of state. For this purpose we have computed the pressure P_p using the density-dependent effective pair potentials between $L = 2000$ SAW polymer coils reported in ref 39 which provide a good fit of the MC data up to $\varphi_p = 2$. These effective polymer−polymer pair potentials are roughly Gaussian in shape, with an amplitude of order $2k_BT$ and a width of order R_g, and vary slowly with density. They serve as input in the compressibility equation within the hypernetted chain (HNC) integral equation,[38] which is quasi-exact for such soft potentials.[12,40] The results have been fitted to the expression

$$Z_p \equiv \frac{\beta P_p}{\rho_p} = 1 + \varphi_p h(\varphi_p); \quad h(\varphi_p) = a(1 + b\varphi_p + c\varphi_p^2)^\alpha \tag{3.3}$$

where we have chosen $\alpha = (1 - 3\nu/2)/(3\nu - 1) \simeq 0.156$. This ensures that the equation of state satisfies the correct asymptotic scaling $Z_p \sim \varphi_p^{1/(3\nu-1)}$ in the semidilute regime.[18] We obtain the coefficients: $a = 1.42143$, $b = 1.12099$, $c = 3.51836$. Expression 3.3 agrees with recent, monomer-level MC simulation data[41] and with the equation of state that has been obtained by resumming the fourth-order virial expansion[42] (relative differences are less than 1.5%). The free energy per polymer follows from eq 3.3 by thermodynamic integration:

$$f_{pol}^{(0)}(\rho_p) = x_1[\ln\rho_p + \int_0^{\varphi_p} h(s)\, ds] \tag{3.4}$$

The first-order correction $f^{(1)}$, derived in the Appendix, is proportional to the second virial coefficient B_2 for a colloid−polymer pair (cf. eq 2.4):

$$f^{(1)} = 2B_2\rho x_1 x_2 = \frac{3}{2\pi} A_2 \sqrt{x_1 x_2}\, \varphi_p^{1/2} \varphi_c^{1/2} \tag{3.5}$$

where $\rho = \rho_c + \rho_p = N/V$ is the overall number density of the mixture, while A_2 is the universal ratio (2.5), as calculated in section 2.

The explicit expression of the second-order term $f^{(2)}$ given in the Appendix requires the knowledge of the effective colloid−polymer pair potential and of the colloid−colloid and polymer−polymer pair correlation functions in the decoupled reference system. For the former we used the analytic solution of the Percus−Yevick (PY) equation for hard spheres,[38] while the latter were computed numerically from the polymer−polymer pair potentials, using the (HNC) integral equation. In the latter case we have used the density-dependent potentials reported in ref 39. Note that those expressions are only valid up to $\varphi_p = 2$: for larger values they predict pair potentials that are somewhat larger than those observed in numerical data. To estimate the error we are making for $\varphi_p \geq 2$, we have systematically repeated the calculation, computing $f^{(2)}$ by using the zero-density potential reported in ref 24. No significant difference is observed in the phase diagrams which will be reported below, indicating that the density dependence of the effective polymer−polymer interaction is irrelevant in the calculation of the second-order term $f^{(2)}$.

Note that, in the limit $\lambda \to 0$, the Mayer function $f(r) = \exp(-\beta v_2(r)) - 1$ reduces to $-\beta v_2(r)$, so that $f^{(1)}$ goes over to the simple random-phase approximation (RPA):

$$f^{(1)} = \rho x_1 x_2 \int d^3\mathbf{r}\, \beta v_2(r) \tag{3.6}$$

Using the overall density ρ (or, equivalently, the volume per particle $v \equiv 1/\rho$) and the polymer number fraction x_1 as independent variables, the spinodal line of a possible colloid−polymer phase separation is determined by the condition

$$S(\rho, x_1) = \frac{\partial^2 f}{\partial v^2}\frac{\partial^2 f}{\partial x_1^2} - \left(\frac{\partial^2 f}{\partial v \partial x_1}\right)^2 = 0 \tag{3.7}$$

The binodal lines are instead determined by imposing equal chemical potentials and equal pressure in the coexisting phases.

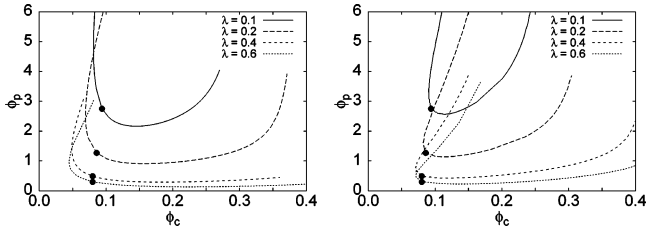

Figure 11. Binodal (left) and spinodal (right) curves for $\lambda = 0.1$, 0.2, 0.4, and 0.6. They are obtained by using thermodynamic perturbation theory based on the Mayer *f*-function. The black circles correspond to the critical points.

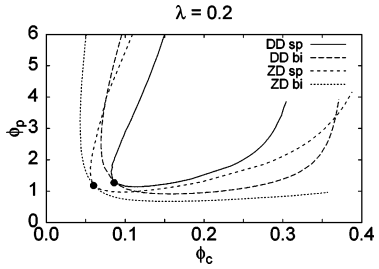

Figure 12. Comparison of the results obtained by using density-dependent (DD) and zero-density (ZD) polymer−polymer potentials. We report the binodals (bi) and the spinodals (sp) for $\lambda = 0.2$. The black circles correspond to the critical points.

Examples of spinodal curves calculated for size ratios $\lambda = 0.1$, 0.2, 0.4, and 0.6 are shown in Figure 11 in the (φ_p, φ_c) plane. As expected the spinodal curve is shifted to higher and higher volume fractions of the two components as the size ratio decreases, since no phase separation will occur in the limit $\lambda \to 0$. For $\lambda = 0.2$ we have repeated the calculation, using the polymer equation of state derived from the zero-density limit of the effective polymer−polymer pair potential evaluated in the scaling limit.[24] This may be regarded as more consistent since the effective colloid−polymer pair potential has been calculated under the same ($\rho \to 0$, $L \to \infty$) conditions. The resulting spinodal and binodal curves turn out to be quite close to those computed by using the density-dependent potentials, see Figure 12. The general trends predicted for the phase behavior of colloid−polymer mixtures with $\lambda < 1$ are not unlike those observed in the MC simulations of Bolhuis et al. (ref 11). In particular, the critical volume fraction of the polymers drops as λ increases while that of the colloids stays nearly constant. However, both critical volume fractions are too low, by roughly a factor of 2 for the polymers and by a factor of 3 for the colloids. These significant discrepancies may be attributed to one (or all) of three reasons. First, the effective colloid−polymer potentials derived in section 2 have been shown to vary significantly with polymer length, particularly so for small λ. The perturbation theory results are based on the scaling limit of these effective potentials, while the MC data of ref 11 are for $L = 2000$. To estimate this effect, we have repeated the calculation for $\lambda = 0.2$ using the zero-density potentials (both for the polymer−polymer free-energy and the polymer-colloid

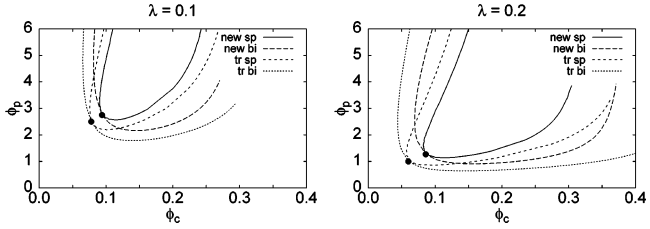

Figure 13. Comparison of results from traditional thermodynamic perturbation theory (tr) and that based on the Mayer *f*-function (new). We report the binodals (bi) and the spinodals (sp) for $\lambda = 0.1$ and $\lambda = 0.2$. The black circles correspond to the critical points.

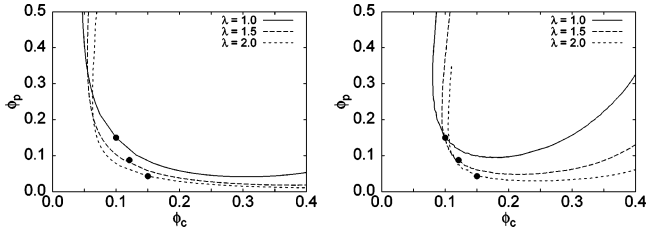

Figure 14. Binodal (left) and spinodal (right) curves for $\lambda = 1$, 1.5, and 2. They are obtained by using thermodynamic perturbation theory based on the Mayer *f*-function. The black circles correspond to the critical points.

perturbative terms) appropriate for $L = 2000$ and compared the results with those obtained using the scaling-limit zero-density potentials (this check cannot be performed by using the density-dependent pair potentials, since we do not have expressions for Z_p accurate enough to distinguish the scaling behavior from that of polymers with $L = 2000$). The spinodal curve changes by a few percent and thus the L dependence cannot explain the large differences we observe.

The second reason for this disagreement may be the neglect of higher-order terms in the perturbative expansion (eq 3.1). Terms beyond $f^{(2)}$ could shift phase coexistence to higher colloid and polymer packing fractions, but this is unlikely at the smallest λ values, where the effective polymer−colloid coupling is weak, so that the perturbative expansion is expected to converge rapidly. This conjecture is confirmed by the comparison of the results with those obtained by using traditional perturbation theory (see the expansion reported in the Appendix corresponding to $w(r; \lambda) = \lambda v_2(r)$). As can be seen from Figure 13, the two perturbative expansions give similar results, and are both significantly different from those of ref 11. The most likely reason for the disagreement lies in the fact that we have used the zero-density limit of the effective colloid−polymer potential while phase separation is observed in the semidilute polymer regime ($\varphi_p \gtrsim 1$) and for finite colloid packing fractions. In the semidilute regime, the relevant polymer length scale is no longer R_g but rather the correlation length $\xi < R_g$, which controls, inter alia, the work of insertion of a colloid when $\lambda \ll 1$.[23,37] This suggests that the second virial coefficient B_2 of a colloid−polymer pair is reduced; such a reduction would imply that higher densities would be required to drive phase separation, in qualitative agreement with the simulation data.

As λ is further increased, we enter the colloid regime. Spinodal and binodal curves, calculated from second-order perturbation theory for $\lambda = 1$, 1.5, and 2 are shown in Figure 14. With increasing λ the critical polymer packing fraction drops steadily, while the critical colloid packing fraction increases slowly in qualitative agreement with the simulation data of ref 15. While the predicted critical φ_c are in reasonable agreement with the latter data, perturbative theory predicts critical φ_p values which are typically a factor of 4 too low. Since both the MC simulations and the perturbation theory are based on the same effective two-component model, the discrepancies must be attributed, in the colloid regime, to the neglect of higher-order terms $f^{(n)}$ ($n \geq 3$) in the free-energy expansion. This conjecture is confirmed by the relative importance of the corrections $f^{(1)}$ and $f^{(2)}$: while in the protein limit $f^{(2)}$ is smaller than $f^{(1)}$ along the binodal curve, this is no longer true in the colloid regime. For instance, at the critical point $f^{(2)}/f^{(1)} \simeq 0.4$, 1, and 1.3 for $\lambda = 0.4$, 1, and 2. Note also that no phase transition at all is predicted for $\lambda \lesssim 2$ when the free-energy expansion (3.1) is truncated after first, rather than second order.

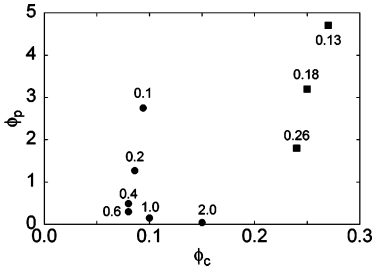

Figure 15. Position of the critical points for several values of λ: circles correspond to the results of the present paper, squares correspond to the Monte Carlo results of ref 11. The number close to each point gives the value of λ.

Figure 15, where we report the critical values of φ_p and φ_c, summarizes our findings relative to the available simulation data of ref 11.

IV. Conclusions

In this paper we have addressed the problem of mixtures of interacting polymers and spherical colloidal particles over a wide range of size ratios λ, covering both the *protein* ($\lambda < 1$) and *colloid* ($\lambda > 1$) regimes which had generally been considered separately so far. Within a general coarse-graining strategy, which has recently proved very successful in the statistical description of dilute and semidilute polymeric systems, we have first determined the effective interaction potential $v_2(r)$ between the centers of mass of an isolated colloid−polymer pair by extensive MC simulations ove a wide range of size ratios $0.02 \leq \lambda \leq 10$. Simulation carried out for several polymer lengths $250 \leq L \leq 64000$ allowed the data to be extrapolated to the scaling limit, using a proper finite-size scaling analysis.[24] A similar analysis was applied to the universal ratio (2.5) involving the second virial coefficient B_2 of a colloid−polymer pair.

The main findings for SAW polymers ($\beta^* = 0$) are the following. The repulsive pair potential $v_2(r)$ is a monotonically decreasing function of the CM-CM distance r and its amplitude $v_2(r = 0)$, which is related to the insertion free energy of a small colloid into a single polymer coil, grows steadily with λ, and exceeds k_BT for $\lambda > 0.2$. For $\lambda > 1$ the potential develops a repulsive core reflecting the fact that a polymer coil has a very low probability of wrapping around a colloidal particle of radius $R_c > R_g$. The L dependence of the effective potential, which is substantial for small λ, becomes insignificant for $\lambda \gtrsim 0.5$.

The second virial coefficient, in its dimensionless universal form A_2, goes through a minimum around $\lambda \gtrsim 0.4$. Both the initial decrease and the asymptotic increase at large λ can be understood in terms of simple scaling arguments.

We have extended the MC calculations to the case where an attraction $-\epsilon$ is added between adjacent nonbonded monomers, to account for solvent quality. The resulting effective colloid−polymer pair potential $v_2(r)$ turns out to be surprisingly insensitive to the reduced inverse temperature $\beta^* \equiv \epsilon/k_BT$, up

to the Θ point, except for the lowest size ratios $\lambda \lesssim 0.5$. The effective potentials near Θ-point conditions are very close to those derived for ideal (noninteracting) polymer chains. The reduced second virial coefficient A_2 increases with β^* for all size ratios, and goes through a minimum at roughly the same value of λ, irrespective of the value of β^*.

The zero-density effective pair potentials are the main input in our investigation of colloid−polymer phase separation over an extended range of size ratios λ. The weakness of the colloid−polymer coupling in the protein limit suggests the use of standard thermodynamic perturbation theory for the calculation of the free energy, starting from a decoupled, two-fluid reference system. However, as λ increases, the effective coupling becomes stronger and develops a highly repulsive core, which renders the standard (Zwanzig) version of thermodynamic perturbation theory inapplicable. We have developed an alternative version, involving an expansion in powers of the Mayer *f*-function, rather than the potential, which applies to any value of λ, and reduces to the Zwanzig expansion in the low-coupling (protein) limit. The second-order version of this modified perturbation theory was used to predict phase diagrams of colloid−polymer mixtures for $0.1 \le \lambda \le 2$. Contrarily to most earlier work, our unified approach applies to both protein and colloid regimes. While the critical polymer concentration is found to drop monotonically as λ increases, the theory predicts an interesting nonmonotonic variation of the critical colloid concentration, which seems to be correlated with the minimum of the reduced second virial coefficient $A_2(\lambda)$ which controls the first-order contribution $f^{(1)}$ to the free energy. Although the theoretical predictions are in qualitative agreement with recent MC data in the protein range[11] and in the colloid range,[15] there are substantial quantitative differences; in particular, the perturbation theory systematically underestimates the colloid packing fractions at coexistence.

The reasons for these discrepancies are, however, different in the two regimes. In the protein regime, the coexistence densities of the polymers are high ($\varphi_p > 1$), corresponding to the semidilute regime, where the use of zero-density effective colloid−polymer potentials is not justified, due to significant polymer overlap. This difficulty can, in principle, be overcome, by using a multiblob (rather than a single blob) representation of the polymer coils, with blob size comparable to the colloid size, along the lines of the ideas in ref 19. A simple scaling argument shows that the overlap density of blobs is $n^{3\nu-1}$ times higher than $\rho^* = 3/(4\pi R_g^3)$ (where $n = L/l$ is the number of blobs of length l in a polymer of length L), so that the coarse-grained system of blobs remains in the dilute (no overlap) regime up to significantly higher polymer concentrations, justifying the use of zero-density effective blob−blob and blob-colloid interactions. Work along these lines is in progress.

On the other hand, in the colloid regime ($\lambda \gtrsim 1$), the disagreement between theory and simulation is likely to be due to another reason, since the polymer density in the coexisting phases is well below ρ^* so that the use of zero-density effective pair potentials is justified. The discrepancy between theory and simulation of the same coarse-grained model must be traced back to the slow convergence of the perturbation theory in the strong-coupling limit, as illustrated by the relative values of the free-energy contributions $f^{(1)}$ and $f^{(2)}$. Calculation of the third-order term $f^{(3)}$ is feasible but tedious, and is left for future work. In the colloid limit a better reference system might a mixture of hard spheres (colloids) and point particles (polymers) excluded from the spheres. In this case the soft polymer−polymer interaction and the soft tail of the colloid−polymer interaction would be treated as perturbations, along lines similar to those laid out in the Appendix.

It is finally worth noting that attempts to replace the perturbation expansion by fluid integral equations, like HNC,[38] for the calculation of the thermodynamics of the two-component colloid−polymer system fail to predict phase separation at any value of λ. It appears that standard integral equations cannot cope with mixtures of hard (colloids) and soft (polymers) particles. It is likely that hybrid integral equations, like those of Rogers and Young (ref 43) would yield more satisfactory results.

The present investigation was restricted to *gas−liquid* coexistence, but could well be extended to include also crystallization of colloid−polymer mixtures in order to map out the full phase diagram.

Appendix A: Thermodynamic Perturbation Theory for a Weakly Coupled Binary Mixture

Consider a binary mixture of N_α particles of species α ($\alpha = A, B$); $N = N_A + N_B$ and $\rho_\alpha = N_\alpha/V$ is the number density of species α. The configuration integral reads:

$$Z(N_A, N_B, V,\beta) = \frac{1}{V^{N_A+N_B}} \int \prod_{i\in A, j\in B} d^3\mathbf{r}_i\, d^3\mathbf{s}_j \exp[-\beta(V_{AA} + V_{BB} + V_{AB})] \quad \text{(A1)}$$

where $V_{\alpha\gamma}$ denotes the total potential energy of interaction between particles of species α and γ. If the two species are decoupled, $V_{AB} \equiv 0$, then

$$Z(N_A, N_B, V,\beta) = Z^{(0)}(N_A, N_B, V,\beta) \equiv Z^{(A)}(N_A, V,\beta) Z^{(B)}(N_B, V,\beta) \quad \text{(A2)}$$

where $Z^{(A)}$ and $Z^{(B)}$ are the configurational integrals for systems *A* and *B*, and the superscript (0) denotes the reference system. The excess free energy of the reference system is

$$F^{(0)} = -k_B T \ln Z^{(0)} = F_A(N_A, V,\beta) + F_B(N_B, V,\beta) \quad \text{(A3)}$$

Now, turn on the coupling between the two species adiabatically by considering intermediate systems in which the two species interact through an interpolating potential $W_{AB}(\lambda)$, $0 \le \lambda \le 1$, such that $W_{AB}(1) = V_{AB}$ and $W_{AB}(0) = 0$. The corresponding configurational integral becomes

$$Z(\lambda) = \frac{1}{V^{N_A+N_B}} \int \prod_{i\in A, j\in B} d^3\mathbf{r}_i\, d^3\mathbf{s}_j \exp[-\beta(V_{AA} + V_{BB} + W_{AB}(\lambda))] \quad \text{(A4)}$$

The corresponding excess free energy is $F(\lambda) = -k_B T \ln Z(\lambda)$. We then adopt the standard procedure of thermodynamic perturbation theory[38] to derive the exact expression:

$$\beta F = \beta F(\lambda = 1) = \beta F^{(0)} + \int_0^1 d\lambda \left\langle \beta \frac{dW_{AB}}{d\lambda} \right\rangle_\lambda \quad \text{(A5)}$$

where $\langle\cdot\rangle_\lambda$ denotes a statistical average over an ensemble of systems characterized by coupling λ [cf. eq A4]. A Taylor expansion of $\langle \beta W'_{AB}\rangle_\lambda$ in powers of λ leads to the series:

$$\beta F = \beta F^{(0)} + \beta\langle W'_{AB}\rangle_0 + \frac{\beta}{2}\langle W''_{AB}\rangle_0 + \frac{\beta^2}{2}(\langle (W'_{AB})^2\rangle_0 - \langle W'_{AB}\rangle_0^2) + \cdots \quad \text{(A6)}$$

Now assume that $W_{AB}(\lambda)$ is pairwise additive so that

$$\beta W_{AB}(\lambda) = \sum_{i=1}^{N_A}\sum_{j=1}^{N_B} w_{AB}(|\mathbf{r}_i - \mathbf{s}_j|;\lambda) \tag{A7}$$

and $w_{AB}(r;\lambda) \approx \lambda w_{AB,0}(r) + \lambda^2 w_{AB,1}(r)/2 + O(\lambda^3)$. It follows

$$\langle \beta W_{AB}' \rangle_0 = N_A N_B \langle w_{AB,0}(|\mathbf{r}_1 - \mathbf{s}_1|)\rangle_0 = N x_A x_B \rho \int \mathrm{d}^3\mathbf{r}\, w_{AB,0}(r) \tag{A8}$$

since A and B particles are uncorrelated in the reference system; in eq A8, $\rho = \rho_A + \rho_B$, while $x_\alpha = \rho_\alpha/\rho = N_\alpha/N$. Therefore

$$f^{(1)} = x_A x_B \rho \int \mathrm{d}^3\mathbf{r}\, w_{AB,0}(r) \tag{A9}$$

Analogously we obtain

$$\langle \beta W_{AB}'' \rangle_0 = N_A N_B \langle w_{AB,1}(|\mathbf{r}_1 - \mathbf{s}_1|)\rangle_0 = N x_A x_B \rho \int \mathrm{d}^3\mathbf{r}\, w_{AB,1}(r) \tag{A10}$$

The second-order term in the series (A6) involves also the square of (A8) subtracted from

$$\langle (\beta W_{AB}')^2 \rangle_0 = \sum_i^{N_A}\sum_j^{N_B}\sum_k^{N_A}\sum_l^{N_B} \langle w_{AB,0}(|\mathbf{r}_i - \mathbf{s}_j|) w_{AB,0}(|\mathbf{r}_k - \mathbf{s}_l|)\rangle_0 \tag{A11}$$

In this quadruple sum, we distinguish four cases: (i) $i = k$, $j = l$; (ii) $i = k$, $j \neq l$; (iii) $i \neq k$, $j = l$; (iv) $i \neq k$, $j \neq l$. Case i gives immediately

$$N_A N_B \langle w_{AB,0}(|\mathbf{r}_1 - \mathbf{s}_1|)^2 \rangle_0 = N x_A x_B \rho \int \mathrm{d}^3\mathbf{r}\, w_{AB,0}(r)^2 \tag{A12}$$

Case ii yields

$$\begin{aligned} &N_A N_B (N_B - 1)\langle w_{AB,0}(|\mathbf{r}_1 - \mathbf{s}_1|) w_{AB,0}(|\mathbf{r}_1 - \mathbf{s}_2|)\rangle_0 \\ &\quad = N_A \rho_B{}^2 \int \mathrm{d}^3\mathbf{s}_1\, \mathrm{d}^3\mathbf{s}_2\, w_{AB,0}(s_1) w_{AB,0}(s_2) g_{BB}{}^{(0)}(|\mathbf{s}_1 - \mathbf{s}_2|) \\ &\quad = N_A \rho_B{}^2 \left[\left(\int \mathrm{d}^3\mathbf{s} w_{AB,0}(s)\right)^2 + \int \frac{\mathrm{d}^3\mathbf{k}}{(2\pi)^3} \hat{w}_{AB,0}(k)^2 \hat{h}_{BB}{}^{(0)}(k) \right] \end{aligned} \tag{A13}$$

where $w_{AB,0}(k)$ and $\hat{h}_{BB}^{(0)}(k)$ are the Fourier transforms of the potential $w_{AB,0}(r)$ and of the pair correlation function $h_{BB}{}^{(0)}(r) = g_{BB}{}^{(0)}(r) - 1$ between particles of species B in the reference system and we have used the convolution theorem. Contribution iii is simply obtained from ii by exchanging A and B:

$$N_B \rho_A{}^2 \left[\left(\int \mathrm{d}^3\mathbf{s}\, w_{AB,0}(s)\right)^2 + \int \frac{\mathrm{d}^3\mathbf{k}}{(2\pi)^3} \hat{w}_{AB,0}(k)^2 \hat{h}_{AA}{}^{(0)}(k) \right] \tag{A14}$$

Finally, contribution iv becomes

$$\begin{aligned} &N_A(N_A - 1) N_B (N_B - 1)\langle w_{AB,0}(|\mathbf{r}_1 - \mathbf{s}_1|) w_{AB,0}(|\mathbf{r}_2 - \mathbf{s}_2|)\rangle_0 = \\ &\quad \rho_A{}^2 \rho_B{}^2 V \left\{ \int \frac{\mathrm{d}^3\mathbf{k}}{(2\pi)^3} \hat{w}_{AB,0}(k)^2 \hat{h}_{AA}{}^{(0)}(k) \hat{h}_{BB}{}^{(0)}(k) + \right. \\ &\quad V[\int \mathrm{d}^3\mathbf{r}\, w_{AB,0}(r)]^2 + [\int \mathrm{d}^3\mathbf{r}\, w_{AB,0}(r)]^2 \int \mathrm{d}^3\mathbf{r}\, [h_{AA}{}^{(0)}(r) + \\ &\quad \left. h_{BB}{}^{(0)}(r)] \right\} \end{aligned} \tag{A15}$$

Gathering results, the second-order term in eq A6 may be cast in the form

$$\begin{aligned} f^{(2)} = &-\frac{1}{2}\left\{ \rho^3 x_A{}^2 x_B{}^2 \left[\int \frac{\mathrm{d}^3\mathbf{k}}{(2\pi)^3} \hat{w}_{AB,0}(k)^2 \hat{h}_{AA}{}^{(0)}(k) \hat{h}_{BB}{}^{(0)}(k) + \right. \right. \\ &\left. \hat{w}_{AB,0}(k=0)^2 (\hat{h}_{AA}{}^{(0)}(k=0) + \hat{h}_{BB}{}^{(0)}(k=0)) \right] + \\ &\rho x_A x_B \left[\int \mathrm{d}^3\mathbf{r}\, [w_{AB,0}(r)^2 - w_{AB,1}(r)] + \rho \hat{w}_{AB,0}(k=0)^2 + \right. \\ &\left. \left. \int \frac{\mathrm{d}^3\mathbf{k}}{(2\pi)^3} \hat{w}_{AB,0}(k)^2 (\rho_A \hat{h}_{AA}{}^{(0)}(k) + \rho_B \hat{h}_{BB}{}^{(0)}(k)) \right] \right\} \end{aligned} \tag{A16}$$

In the case under consideration in this paper, the A and B species are the colloids and the polymers. We consider two different interpolating potentials. A first possibility is $W_{AB}(\lambda) = \lambda V_{AB}$, which corresponds to the traditional Zwanzig perturbation theory.[38] In this case $w_{AB,0}(r) = \beta v_{AB}(r)$ and $w_{AB,1} = 0$. Zwanzig theory is inapplicable when $v_{AB}(r)$ contains a hard-core repulsion, as is the case for colloid−polymer mixtures with $\lambda \gtrsim 1$. A second possibility is to interpolate between zero and full $A-B$ interaction following the path ($0 \leq \lambda \leq 1$):

$$\mathrm{e}^{-\beta W_{AB}(\lambda)} = \prod_{i=1}^{N_A}\prod_{j=1}^{N_B} [1 + \lambda f_{AB}(|\mathbf{r}_i - \mathbf{s}_j|)] \tag{A17}$$

where $f_{AB}(|\mathbf{r}_i - \mathbf{s}_j|) = \exp[-\beta v_{AB}(|\mathbf{r}_i - \mathbf{s}_j|) - 1$ is the Mayer function, which is finite whatever the strength of the repulsion. Taking logarithms of both sides of eq A17, we find in this case $w_{AB,0}(r) = -f_{AB}(r)$ and $w_{AB,1}(r) = f_{AB}(r)^2$. Substitution into eqs A9 and A16 leads to the free-energy expansion used in the calculations presented in this paper.

Note that the two expansions coincide in the limit $v_{AB} \to 0$, up to terms of order $v_{AB}{}^3$, since in this case $f_{AB}(r) \simeq -v_{AB}(r)$. Thus, in the calculations presented in this paper the difference in the results obtained at the same densities by using the two different expansions should decrease as $\lambda \to 0$, since in this limit $v_{AB} \to 0$.

References and Notes

(1) Asakura, S.; Oosawa, F. *J. Chem. Phys.* **1954**, *22*, 1255.
(2) Vrij, A. *Pure Appl. Chem.* **1976**, *48*, 471.
(3) For reviews, see, e.g.: Likos, C. N. *Phys. Reports* **2001**, *348*, 267. Hansen, J.-P.; Löwen, H. in *Bridging Times Scales: Molecular Simulations for the Next Decade*; Nielaba, P., Mareschal, M., Ciccotti, G., Eds.; Springer: Berlin, 2002.
(4) Abbott, N. L; Blankschtein, D.; Hatton, T. A. *Macromolecules* **1992**, *25*, 5192.
(5) Tuinier, R.; Dhont, J. K. G.; De Kruif, C. G. *Langmuir* **2000**, *16*, 1497.
(6) Clegg, S. M.; Williams, P. A.; Warren, P. B.; Robb, I. D. *Langmuir* **1994**, *10*, 3390.
(7) Hennequin, Y.; Evens, M.; Quezada Angulo, C. M.; van Duijneveldt, J. S. *J. Chem. Phys.* **2005**, *123*, 054906. Zhang, Z.; van Duijneveldt, J. S. *Langmuir* **2006**, *22*, 63.
(8) See ref 37 and references therein; for a recent review see: Eisenriegler, E. In *Soft Condensed Matter*; Gompper, G., Schick, M., Eds.; Wiley VCH: Weinheim, Germany, 2005.
(9) For a review, see: Fuchs, M.; Schweizer, K. S. *J. Phys.: Condens. Matter* **2002**, *14*, R239.
(10) Meijer E. J.; Frenkel, D. *J. Chem. Phys.* **1994**, *100*, 6873.
(11) Bolhuis, P. G.; Meijer, E. J.; Louis, A. A. *Phys. Rev. Lett.* **2003**, *90*, 068304.
(12) Bolhuis, P. G.; Louis, A. A.; Hansen, J. P.; Meijer, E. J. *J. Chem. Phys.* **2001**, *114*, 4296.
(13) Asakura, S.; Oosawa, F. *J. Polym. Sci., Polym. Symp.* **1958**, *33*, 183.
(14) Krakoviack, V.; Hansen, J. P.; Louis, A. A. *Phys. Rev. E* **2003**, *67*, 041801.
(15) Bolhuis, P. G.; Louis, A. A.; Hansen, J. P. *Phys. Rev. Lett.* **2002**, *89*, 128302.
(16) Moncho-Jordá, A.; Louis, A. A.; Bolhuis, P. G.; Roth, R. *J. Phys.: Condens. Matter* **2003**, *15*, S3429.

(17) Lekkerkerker, H. N. W.; Poon, W. C. K.; Pusey, P. N.; Stroobanks, A.; Warren, P. B. *Europhys. Lett.* **1992**, *20*, 559.
(18) de Gennes, P. G. *Scaling Concepts in Polymer Physics*; Cornell University Press: Cornell, NY, 1979.
(19) Sear, R. P. *Phys. Rev. Lett.* **2001**, *86*, 4696. Sear, R. P. *Phys. Rev. E* **2003**, *66*, 051401.
(20) Gast, A. P.; Hall, C. K.; Russel, W. B. *J. Colloid Interface Sci.* **1983**, *96*, 251.
(21) Rotenberg, B.; Dzubiella, J.; Hansen, J. P.; Louis, A. A. *Mol. Phys.* **2004**, *102*, 1.
(22) Odijk, T. *J. Chem. Phys.* **1997**, *106*, 3402.
(23) de Gennes, P. G. *C. R. Acad. Sci. Paris B* **1979**, *288*, 359.
(24) Pelissetto, A.; Hansen, J. P. *J. Chem. Phys.* **2005**, *122*, 134904.
(25) For a review, see: Pelissetto, A.; Vicari, E. *Phys. Rep.* **2002**, *368*, 549.
(26) Grassberger, P.; Hegger, R. *J. Chem. Phys.* **1995**, *102*, 6881. Grassberger, P. *Phys. Rev. E* **1997**, *56*, 3682.
(27) Nickel, B. G. *Macromolecules* **1991**, *24*, 1358.
(28) Li, B.; Madras, N.; Sokal, A. D. *J. Stat. Phys.* **1995**, *80*, 661.
(29) Lal, M. *Mol. Phys.* **1969**, *17*, 57.
(30) MacDonald, B.; Jan, N.; Hunter, D. L.; Steinitz, M. O. *J. Phys. A: Math. Gen.* **1985**, *18*, 2627.
(31) Madras, N.; Sokal, A. D. *J. Stat. Phys.* **1988**, *50*, 109.
(32) Sokal, A. D. in *Monte Carlo and Molecular Dynamics Simulations in Polymer Science*; Binder, K., Ed.; Oxford University Press: Oxford, U.K., 1995.
(33) Caracciolo, S.; Causo, M. S.; Ferraro, G.; Papinutto, M.; Pelissetto, A. *J. Stat. Phys.* **2000**, *100*, 1111. Caracciolo, S.; Papinutto, M.; Pelissetto, A. *Phys. Rev. E* **2002**, *65*, 031106.
(34) Geyer, C. J. Markov Chain Monte Carlo Maximum Likelihood. In *Computer Science and Statistics: Proceedings of the 23rd Symposium on the Interface*; Keramidas, E. M., Ed.; Interface Foundation: Fairfax Station, VA, 1991; p 156.
(35) Tesi, M. C.; van Rensburg, E. J. J.; Orlandini, E.; Whittington, S. G. *J. Stat. Phys.* **1996**, *82*, 155.
(36) Tuinier, R. *Eur. Phys. J. E* **2003**, *10*, 123.
(37) Eisenriegler, E. *J. Chem. Phys.* **2000**, *113*, 5091.
(38) Hansen J. P.; McDonald, I. R. *Theory of Simple Liquids*, 3rd ed.; Academic: Amsterdam, 2006.
(39) Bolhuis, P. G.; Louis, A. A. *Macromolecules* **2002**, *35*, 1860.
(40) Likos, C. N.; Lang, A.; Watzlawek, M.; Löwen, H. *Phys. Rev. E* **2001**, *63*, 031206.
(41) Addison, C. I.; Hansen, J. P.; Louis, A. A. *J. Chem. Phys.* **2004**, *121*, 612.
(42) Caracciolo, S.; Mognetti, B. M.; Pelissetto, A. *J. Chem. Phys.* **2006**, *125*, 094903.
(43) Rogers, F. J.; Young, D. A. *Phys. Rev. A* **1984**, *30*, 999.

MA061690F